EVALUATION OF SOIL MOISTURE SENSING TECHNOLOGIES IN SILT LOAM AND LOAMY SAND SOILS: ASSESSMENT OF PERFORMANCE, TEMPERATURE SENSITIVITY, AND SITE- AND SENSOR-SPECIFIC CALIBRATION FUNCTIONS

K. Sharma, S. Irmak, M. S. Kukal, M. C. Vuran, A. Jhala, X. Qiao

HIGHLIGHTS

- Nine soil moisture sensors were evaluated in two soil types under different installation orientations.
- Sensor-specific and soil-specific calibration functions were developed and validated.
- Sensor performance improved substantially (31% to 89%) after calibration.
- On average, sensor performance was 67% better in loamy sand than in silt loam soil.

ABSTRACT. *Reliable soil moisture information is vital for optimal irrigation management, farm-level agronomic decision-making, hydrologic studies, and cropping systems modeling. A wide range of soil moisture sensing technologies is commercially available, but their performance must be evaluated for diverse conditions of use. In this research, we investigated nine soil moisture sensors based on time-domain reflectometry, capacitance, and electrical resistance principles in production field conditions with two installation orientations, i.e., vertical (V) and horizontal (H), in two soils (silt loam and loamy sand) and two growing seasons (2017 and 2018). Performance parameters deduced from the 2017 datasets revealed that sensor type and soil type significantly affected the soil moisture sensor performance under factory calibration (F.C.); however, sensor installation orientation did not. Thus, the sensors were only evaluated based on their performance in horizontal orientation in both soils. Precision and accuracy were considered targets to assist in appropriate sensor selection. To improve sensor accuracy, site-specific calibration (S.S.C.) functions were developed and validated using independent datasets from 2018. Considering mean bias error (MBE), all sensors overestimated volumetric soil water content (θ_v) in both soils, with the exception of TEROS 21 (MPS-6) in silt loam and JD probe in loamy sand. On average, sensor performance was 67% better in loamy sand than in silt loam. Overall, the sensors showed higher precision in silt loam (R^2 = 0.53 to 0.93) than in loamy sand (R^2 = 0.25 to 0.82). Substantial post-S.S.C. improvement (32% to 89%) was observed in all sensors' performance relative to F.C. in silt loam. In loamy sand, while most sensors performed reasonably well with F.C., considerable improvements (28% to 85%) were observed with S.S.C. Significant differences ($p < 0.05$) were observed in sensors' sensitivity to soil temperature (T_{soil}), which ranged from 14°C to 23°C in silt loam and from 14°C to 25°C loamy sand during the experiments. The CS655, 10HS, 5TE, and TEROS 21 (MPS-6) sensors showed significant ($p < 0.05$) sensitivity to T_{soil} fluctuations, with T_{soil} explaining a maximum of 17% of the variance observed in sensor performance. No statistically significant ($p > 0.05$) sensitivity was detected for any of the sensors in loamy sand. TEROS 21 (MPS-6) had the highest sensitivity to T_{soil} with a slope of -4.25. In contrast, while statistically significant ($p < 0.05$), 5TE was the least sensitive to T_{soil} variability with a slope of 1.81. The information, data, and analyses presented here can be instrumental for informed sensor selection and use in decision-making in production fields with similar soil textures and soil water regimes.*

Keywords. *Capacitance, Irrigation, Sensors, Site-specific calibration, Soil moisture, TDR, Time-domain reflectometry.*

Submitted for review on 21 May 2020 as manuscript number ITSC 14112; approved for publication as a Research Article by the Information Technology, Sensors, & Control Systems Community of ASABE on 3 February 2021.

The authors are **Kiran Sharma,** Global Technical Support Engineer, Lindsay Corporation, Omaha, Nebraska (formerly MS Student in the Irmak Research Laboratory at the University of Nebraska-Lincoln (UNL) under the supervision of Professor Suat Irmak); **Suat Irmak,** Professor and Department Head, Department of Agricultural and Biological Engineering, Pennsylvania State University, University Park, Pennsylvania (formerly University of Nebraska-Lincoln, Lincoln, Nebraska); **Meetpal S. Kukal,** Assistant Research Professor, Department of Agricultural and Biological Engineering, Pennsylvania State University, University Park, Pennsylvania (formerly MS and PhD student and Post-Doctoral Research Associate in the Irmak Research Laboratory under the supervision of Suat Irmak); **M. Can Vuran,** Professor, Department of Computer Science and Engineering, UNL; **Amit Jhala,** Associate Professor, Department of Agronomy and Horticulture, UNL; **Xin Qiao,** Assistant Professor, Panhandle Research and Extension Center, UNL, Scottsbluff, Nebraska. **Corresponding author:** Suat Irmak, 105 Agricultural Engineering Building, Pennsylvania State University, University Park, PA 16802; phone: 814-865-7792; e-mail: sfi5068@psu.edu.

Soil moisture in the zone of aeration dictates transpiration and evaporation processes, plant growth (Romano, 2014), and a multitude of ecological, hydrological, geotechnical, and meteorological processes

Vol. 64(4): 1123-1139 ISSN 2151-0032 https://doi.org/10.13031/trans.14112

(Schmugge et al., 1980). In agricultural production, accurate soil moisture information contributes to optimum irrigation decision-making, reducing the costs incurred from over-irrigation, such as increased fertilizer use, pumping, and undesirable nitrate leaching and greenhouse gas emissions (Doorenbos and Kassam, 1979). On the other hand, insufficient or inaccurate soil moisture information makes it equally likely to under-irrigate, and there is strong evidence that both over- and under-irrigation result in yield penalties (Doorenbos and Kassam, 1979; Irmak, 2014) in a wide range of crops (beans, cotton, groundnut, maize, potato, soybean, sugarcane, sunflower, spring wheat, and winter wheat). Apart from assisting in irrigation decisions, accurate soil moisture measurement aids in determining optimum planting time, machinery use, plant root-zone water status, crop water use (evapotranspiration, ET_c), soil water balance analyses, and crop modeling (Ochsner et al., 2013). Farmers are challenged to consume water resources more efficiently while meeting crop water requirements to achieve optimum productivity (Irmak, 2010). In light of these challenges, use of soil moisture measurements in production decisions could lead to 40% improvement in water use efficiency (Irmak et al., 2012).

Several direct and indirect methods have been developed in recent decades to estimate volumetric soil water content (θ_v). Direct methods include the gravimetric method, and indirect methods include neutron scattering, tensiometry, gamma attenuation, electromagnetic (EM) technology, resistive sensors, time-domain reflectometry (TDR), capacitance-type devices, infrared method, global positioning systems, remote sensing, and cosmic ray neutron method (Irmak, 2019a, 2019b; Romano, 2014; Schmugge et al., 1980; Zazueta and Xin, 1994). Soil moisture sensors have been shown to vary in their performance with several confounding factors that include the soil type, soil chemical and physical properties, soil temperature, and soil moisture range in which they operate (Irmak and Irmak, 2005). The gravimetric method has been considered the most accurate θ_v measurement technique, if the soil sampling procedure is practiced accurately (Reynolds, 1970). All other sensing techniques have been developed using validation data from this method. However, the gravimetric method involves rigorous soil sampling and drying time, and hence an unavoidable delay until the soil moisture is determined, rendering it unsuitable for real-time or near-real-time decision making, especially when frequent measurements are required (daily, sub-daily, etc.). These challenges are met somewhat successfully by the neutron scattering method, which has been shown to accurately and precisely estimate θ_v and hence replace the need for the gravimetric procedure (Evett et al., 2002, 2003; Hanson and Peters, 2000; Zhu et al., 2019; Leib et al., 2003). Although potentially hazardous radioactive material is involved, and detailed safety training is required, neutron scattering is widely accepted as an accurate reference method to measure θ_v (Evett, 2003; Irmak, 2019a, 2019b).

The largest array of commercially available soil moisture sensors is based on EM sensing of the soil medium. These sensors are categorized as electrical resistivity (ER), TDR, and capacitance-type devices (Heng et al., 2002; Jones et al., 2002). ER sensors provide output in terms of soil matric potential (SMP) by using the sensor matrix's (in equilibrium with the soil) resistive properties (Zazueta and Xin, 1994). Even though they require site-specific calibration (S.S.C.) (Irmak, 2014) and precise and careful calibration to function in sandy soils (Irmak and Haman, 2001), their low cost and ease of use make them desirable. Similarly, TDR and capacitance sensors estimate the apparent dielectric permittivity (ε_{ra}) of the soil (Schmugge et al., 1980), which is calibrated with θ_v. Some studies have investigated the relationships between EM properties (such as ε_{ra}) and θ_v (Topp et al., 1980, 2000).

Nebraska consists of 17 soil series that constitute about 49% of the land area, which demands differential soil moisture sensing (USDA, 2017) and is also the case in most other U.S. states. Among other soil properties such as temperature, salinity, organic matter content, and bulk density, soil texture has been recognized to affect a factory-calibrated sensor's performance in agricultural fields. This is due to the highly controlled factory calibration (F.C.) conditions, such as homogeneous soil materials (usually loams or sands), distilled water, controlled soil temperatures, and uniform soil packing, all of which almost never conform with real application conditions (Hignett and Evett, 2008). These impacts of soil texture on the performance of soil moisture sensors have been addressed by a reasonable body of literature (Paige and Keefer, 2008; Rüdiger et al., 2010; Kelleners et al., 2005; Jacobsen and Schjønning, 1993; Ponizovsky et al., 1999). As the application conditions increasingly deviate from F.C. conditions, the degree of inaccuracy of soil moisture sensor estimations increases. Nevertheless, some soil moisture sensors are attractive to the user community owing to their low cost and ease of operation.

Because soil texture is the primary source of heterogeneity of field-specific conditions, evaluating soil moisture sensors for individual textural classes should be a producer-oriented research theme. Within Nebraska, silt loam and loamy sand soils dominate the agricultural land-use category. To accomplish this research goal, this study focused on two such agricultural fields with silt loam and loamy sand soils. These agricultural fields also account for two different land-use classifications: agricultural row crops (maize and soybean) and rangeland/pastureland, respectively. These two land-use systems account for 33% (6 million ha) and 51% (9 million ha) of the total area of Nebraska's farms and ranches, representing 84% (15 million ha) of all cropland in the state (USDA, 2017). Although land-cover does not influence the performance of soil moisture sensors, it dictates root water extraction patterns that change the moisture regimes observed by a sensor. Moreover, the two land-covers are also different in their soil structure and physical characteristics, given the presence (for the row crop site) and absence (for the pasture site) of tillage practices, differences in soil chemical properties and organic matter content, compaction (bulk density), and other characteristics, representing scenarios that the sensors will ultimately be used in. We selected these conditions to ensure that the research findings can be useful and transferrable to a representative Nebraskan producer, as well as regions beyond Nebraska that have similar soil and vegetation characteristics.

It is critical that sensor evaluation conditions are identical to the conditions of final application, but this criterion is not always met in research. Laboratory (controlled) evaluations of sensors (Baumhardt et al., 2000; Kizito et al., 2008; Vaz et al., 2013; Ojo et al., 2015) yield results that are suitable for homogeneous conditions such as sieved soil, uniform bulk density, minimal spatial attributes in most soil physical, chemical, and hydraulic properties, and non-structured soil. However, in actual field conditions, soil structure, compaction, and non-uniformity in bulk density are common traits. Additionally, it is preferable to study entire growing seasons for data collection to evaluate sensor performance under natural conditions, rather than using imposed drying/wetting cycles (Zhu et al., 2019). These confounding factors were addressed by conducting this research in undisturbed soil in field conditions in two entire growing seasons to allow greater representativeness of the natural field conditions and to capture a wide range of soil moisture in both soils.

In addition to the abovementioned considerations, sensor installation orientation (horizontal vs. vertical placement) remains an issue. Not all commercial sensor manufacturers give recommendations for installation orientation, and thus the relative ease of installation and removal can dictate these decisions. Limited research (Zhu et al., 2019; Plauborg et al., 2005; Caldwell et al., 2018) has shown that sensor installation influences sensor performance. This issue is relevant only for probe-based sensors, as it alters the actual volume of soil sampled by the sensor. Our research aims to fill this gap by evaluating the installation orientations of probe-based sensors in two fields containing two dominant soil textures in Nebraska. Specifically, the objectives of this research were to: (1) evaluate nine commercial EM sensors in silt loam and loamy sand soils when installed in vertical and horizontal orientations, (2) develop calibration functions from data collected during a growing season in the two soil types, (3) evaluate the calibration functions for an independent growing season, and (4) quantify the influence of soil temperature fluctuations on sensor performance.

Materials and Methods

Site and Soil Description

The field experiments were conducted for two growing seasons (2017 and 2018) at two field sites (fig. 1) that represent two predominant soil types in the state. Site 1 is one of the Irmak Research Laboratory's (IRL) advanced irrigation engineering and evapotranspiration research facilities at the University of Nebraska's (UNL) South Central Agricultural Laboratory (SCAL), located near Clay Center, Nebraska (40° 43′ N and 98° 8′ W at an elevation of 552 m above mean sea level). This site is also one of the NEBFLUX (Nebraska Water and Energy Flux Measurement, Modeling, and Research Network; Irmak, 2010) sites that operates ten surface energy balance flux measurement towers for different vegetation surfaces. The long-term (1980 to 2010) average annual precipitation in this area is 730 mm, and the long-term (1980 to 2010) average growing season (May 1 to September 30) precipitation is 437 mm, with significant interannual and inter-growing season variation in both magnitude and timing.

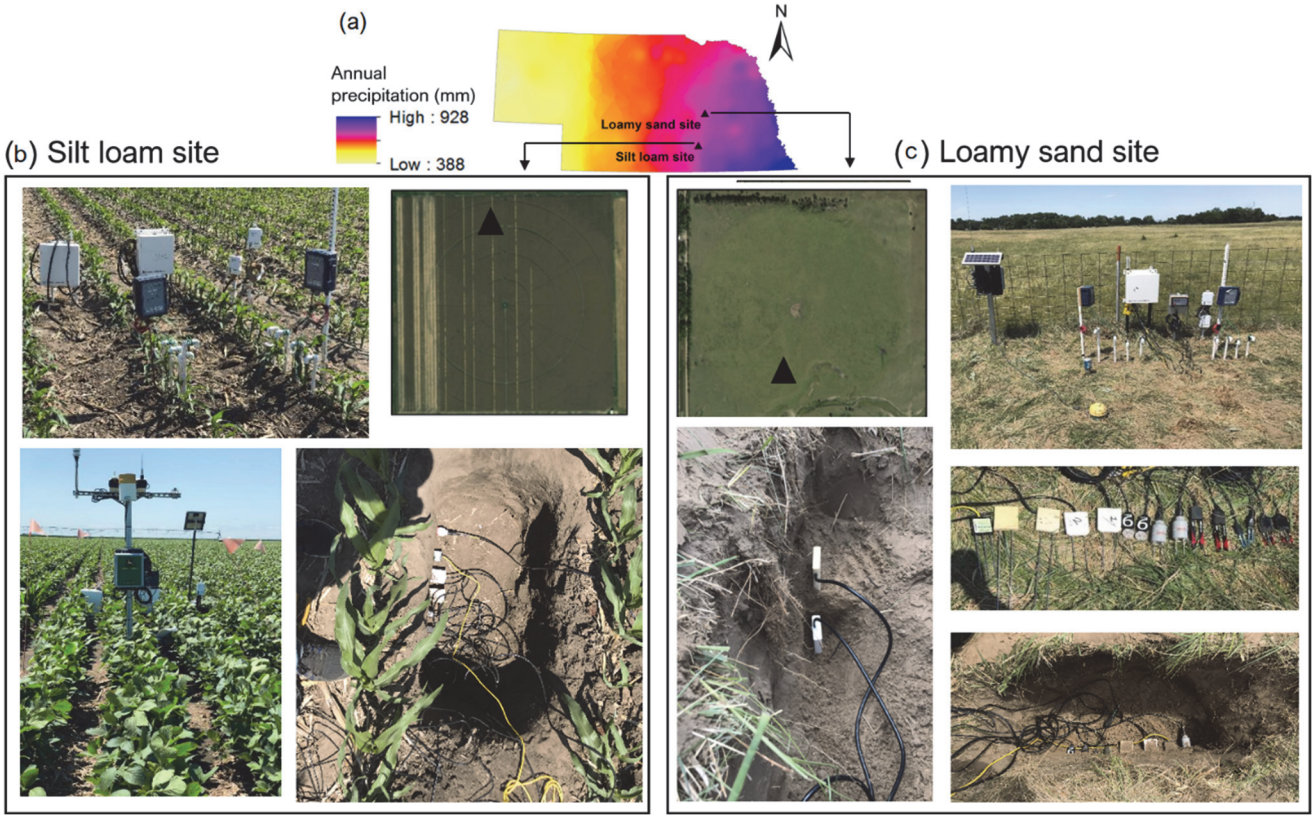

Figure 1. (a) Geographic locations of the two experimental sites in the Irmak Research Laboratory (IRL) research facilities, as shown on a map of Nebraska (the state map also shows the gradient of long-term mean annual precipitation); (b) photos taken during the experimental period at the silt loam site; and (c) photos taken during the experimental period at the loamy sand site.

Site 2 is at Central City, Nebraska (41°16′ N and 97°56′ W at an elevation of 549 m above mean sea level), approximately 10 km north of the Platte River. This site is a rainfed grassland that is approximately 70 ha in size. Site 2 is also one of the NEBFLUX sites that is a part of an investigation of energy balance and productivity of side-by-side rainfed and irrigated grasslands. The long-term (1980 to 2010) average annual precipitation and growing season precipitation are 732 mm and 464 mm, respectively. The soils were characterized for their water retention properties by developing soil water characteristic functions via pressure plate apparatus.

Site 1 has well-drained Hastings silt loam soil (Crete fine, smectitic, mesic Pachic Argiustolls) with a field capacity and permanent wilting point of 0.34 m^3 m^{-3} and 0.14 m^3 m^{-3}, respectively (Irmak, 2010). Site 2 has deep, moderately drained, and moderately permeable loamy sand (Ipage mixed, mesic, Oxyaquic Ustipsamments) with a field capacity and permanent wilting point of 0.19 m^3 m^{-3} and 0.05 m^3 m^{-3}, respectively (Irmak, 2010). Hereafter, we will refer to sites 1 and 2 by their soil types, i.e., silt loam and loamy sand, respectively. Table 1 presents basic soil characteristics for both sites.

Vegetation and Management at Experimental Sites

Silt Loam (Site 1)

At site 1, irrigated row crops were grown during the experimental period. In 2017, field maize (*Zea mays* L.) hybrid G14H66-3010A was grown with a planting rate of 78,620 seeds ha^{-1} and planting depth of 0.06 m. The maize crop was planted on 12 May 2017, emerged on 27 May 2017, and was harvested on 6 November 2017. Similarly, in 2018, soybean (*Glycine max*) Golden Harvest GH3324X variety was grown with a planting rate of 370,700 seeds ha^{-1} and planting depth of 0.03 m. The soybean crop was planted on 8 May 2018, emerged on 17 May 2018, and was harvested on 19 October 2018. The typical effective rooting depth of maize and soybean at the experimental site is 1.50 and 1.20 m, respectively. Total available water-holding capacity of the top 1.50 m soil profile is approximately 300 mm. The field (16.5 ha) was irrigated using a four-span hydraulic and continuous-move center-pivot irrigation system (T-L Irrigation, Hastings, Neb.). The system has a 1.512 m^3 min^{-1} flow rate with a first span length of 48.46 m and second, third, and fourth span lengths of 48.16 m. Irrigation management was conducted to maintain crops at optimum growth conditions and maintain root zone soil water between approximately 90% of field capacity and 55% of total available water (maximum allowable depletion or MAD = 45%). The MAD value was selected based on extensive long-term experiments at SCAL (Irmak, 2015a, 2015b). Irrigations were applied in both growing seasons, totaling 159 mm in 2017 and 64 mm in 2018.

Loamy Sand (Site 2)

Site 2 is a rainfed native grassland that is approximately 70 ha in area and contains primarily buffalograss [*Bouteloua dactyloides* (Nutt.)] (~90%) and tall fescue (*Festuca arundinacea*) (Irmak, 2010). This grassland was established in 1980 and still maintains its natural establishment conditions. Due to the rainfed conditions, the vegetation experiences water stress, especially during July and August when atmospheric moisture demand (vapor pressure deficit), air temperature, and solar radiation are at their maximum. It is grazed throughout most of the growing season (May until October), and the grass height varies between approximately 5 and 13 cm throughout the season (Irmak, 2010).

Soil Moisture Sensors

We used nine different commercial soil moisture sensors that fall into three categories: TDR-based, capacitance-based, and ER-based. At each site, we evaluated two sets of each sensor, one of which was installed in horizontal orientation (parallel to the ground surface) and the other in vertical orientation (perpendicular to the ground surface). The only exceptions were the JD probe, which can only be installed vertically, being a multi-sensor probe, and the TDR-315L, which was only evaluated in horizontal orientation. The following sections briefly describe each sensor evaluated.

TDR-Based Sensors

TDR-315L (Acclima, Meridian, Ida.): This sensor is a waveform digitizing time-domain reflectometer that derives soil permittivity from the propagation time of an EM impulse conveyed along its waveguide. The measured apparent dielectric permittivity (ε_{ra}) is then converted to θ_v using a proprietary dielectric mixing model. In addition to θ_v, the sensor measures soil temperature, soil permittivity, and soil electrical conductivity using the Giese-Tiemann method (Giese and Tiemann, 1975).

CS616 and CS655 (Campbell Scientific, Logan, Utah): These sensors are both water content reflectometers. The CS616 sensor is a transmission line oscillator (TLO) sensor that uses two parallel rods to form an open-ended transmission line or a waveguide. The probe outputs a MHz oscillation frequency, which is scaled down and read by a Campbell Scientific datalogger. The measured oscillation frequency is inversely related to ε_{ra}. The elapsed travel time and ε_{ra} are used to calculate θ_v using Topp's equation (eq. 1) (Topp et al., 1980); θ_v is the main contributor to the ε_{ra} of the soil:

Table 1. Textural and hydraulic properties of experimental soils (ρ_b = bulk density, OMC = organic matter content, PWP = permanent wilting point, and EC = electrical conductivity).

Soil Type	Soil Layer (cm)	Particle Size Distribution: Sand (%)	Silt (%)	Clay (%)	ρ_b (g cm^{-3})	OMC (%)	Field Capacity (m^3 m^{-3})	PWP (m^3 m^{-3})	Saturation (m^3 m^{-3})	Slope (%)	Compaction (kPa)	EC (dS m^{-1})
Silt loam	0-30	18.7	55.6	25.6	1.35	2.81	0.34	0.17	0.50	1.0	0.90	0.35
	30-60	16.2	45.3	38.5	1.13	2	0.38	0.23	0.50			
	60-90	15.8	51	33.2	1.18	1.3	0.36	0.20	0.47			
	90-120	15.8	56.1	28.1	1.24	1.07	0.35	0.17	0.46			
Loamy sand	0-120	77	16	7	1.54	1.1	0.19	0.05	0.42	1.0	0.96	0.13

$$\theta_v = 4.3\times10^{-6}\left(\varepsilon_{ra}{}^3\right) - 5.5\times10^{-4}\left(\varepsilon_{ra}{}^2\right) + 2.92\times10^{-2}\left(\varepsilon_{ra}\right) - 5.3\times10^{-2} \quad (1)$$

The CS655 sensor is also based on CS616 technology, but with improvements in the oscillator circuitry, voltage attenuator, and sensor firmware. The CS616 measures the θ_v of soil, whereas the CS655 measures the electrical conductivity, dielectric permittivity, and temperature, in addition to θ_v.

Capacitance-Based Sensors

5TE, 10HS, and EC-5 (Meter Group, Pullman, Wash.): The 10HS and EC-5 sensors are two-prong devices, while the 5TE is a three-prong device. All three devices use capacitance technology to measure θ_v, which is based on the dielectric constant (ε_r) of the soil. An EM field is produced between the positive and negative plates, and an oscillator operating at 70 MHz is used to measure the dielectric property of the soil. All three sensors estimate θ_v using Topp's equation (eq. 1). Because the ε_r of water is much higher than that of air or soil minerals, the ε_r of the soil is a sensitive measure of θ_v. One of the important differences among these sensors is the volume of influence, as the 10HS has three times the volume of influence of the other two sensors, measuring one liter of soil volume.

SM150 (Delta-T Devices, Cambridge, UK): The SM150 is a two prong-device through which a waveform of 100 MHz is applied that transmits EM waves to the soil. Based on the soil's ε_r, a stable voltage output signal is generated; θ_v is calculated by means of differential analog DC voltage by combining the sensor calibration along with a calibration equation. Equations 2 and 3 (Delta-T, 2016) were used to convert the SM150 readings from mV to θ_v.
For generalized mineral soils:

$$\theta_{v(mineral)} = -0.0714 + 1.7190V - 3.7213V^2 + 5.8402V^3 - 4.3521V^4 + 1.2752\ V^5 \quad (2)$$

For generalized organic soils:

$$\theta_{v(organic)} = -0.0390 + 1.87530V - 4.0596V^2 + 6.3711V^3 - 4.7477V^4 + 1.3911V^5 \quad (3)$$

where V is the SM150 output (mV).

JD Field Connect (John Deere Water, San Marcos, Cal.): The JD Field Connect (hereafter the JD probe) is a multi-depth probe that has capacitors at depths of 10, 20, 30, 50, and 100 cm. The JD probe outputs a count proportional to the sensor circuit (resonant) frequency, which is used to calculate a scaled frequency (SF) ranging between zero and one. The SF is then converted to θ_v using the manufacturer's embedded calibration equation. The JD probe is equipped with an antenna that provides real-time remote data access and a solar panel that recharges the battery.

ER-Based Sensor

TEROS 21 (MPS-6) (Meter Group, Pullman, Wash.): The TEROS 21 (MPS-6) sensor uses porous ceramic discs to determine soil matrix potential (Ψ_m). Post-measurement, we manually converted each Ψ_m measurement to θ_v using soil- and depth-specific moisture characteristic curves developed by Irmak (2019b)) and Irmak et al. (2016).

Reference Soil Moisture Measurement

We used a new neutron probe (NP) soil moisture gauge (model 4302, Troxler Electronic Laboratories, Inc., Research Triangle Park, N.C.) to represent the true θ_v (θ_{vref}) in our research. All other sensors were compared, assessed, and calibrated against the NP. The NP is comprised of a source and detector, which are lowered into aluminum access tubes. These access tubes were installed in the field using a Giddings probe (Giddings Machine Co., Windsor, Colo.). Fast neutrons (approx. 17,000 neutrons per second) are emitted from the source into the soil by a radioactive substance. These neutrons are thermalized by the hydrogen atoms present in the soil-water molecules and slow down. This slowdown of the fast neutrons emitted into the soil is measured by the detector to determine θ_{vref} using a linear calibration equation with slope (a) and intercept (b):

$$\theta_{vref} = a \times \left(\frac{\text{Neutron count}}{\text{Standard count}}\right) + b \quad (4)$$

The standard count was measured prior to each measurement campaign individually at each site. For accurate soil moisture measurements, S.S.C. equations were developed (S. Irmak, unpublished research data) for both sites by correlating the factory-calibrated NP measurements to the θ_v determined using the gravimetric method with a soil sample (fig. 2, eq. 5):

$$y = \begin{cases} 0.9061x + 0.0354 \text{ for silt loam} \\ 1.0848x - 0.0246 \text{ for loamy sand} \end{cases} \quad (5)$$

where y is the F.C. θ_{vref}, and x is the gravimetric θ_v.

Experimental Design and Sensor Installation

The experimental factors were the soil type, sensor orientation, and sensor model. Each sensor was limited to one replication due to the following constraints: (1) using the limited financial investment to include a wider variety of

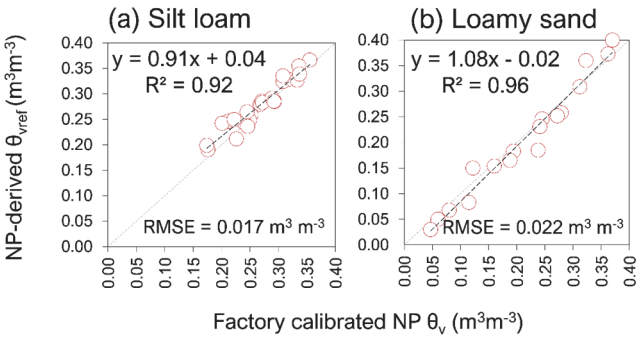

Figure 2. Regression between the Troxler 4302 neutron probe (NP) factory-calibrated volumetric soil-water content and gravimetrically determined volumetric soil water content in the (a) silt loam (SCAL) and (b) loamy sand (Central City) soils. The data points represent spatially distinct, multi-depth (0.30 to 1.80 m) information collected concurrently from NP and gravimetric sampling. Calibration of the neutron probe for both soils was carried out in the Irmak Research Laboratory.

commercial sensors to produce stakeholder-oriented information rather than focusing on a limited number of sensors with more replicates, and (2) the need to minimize the spatial moisture variability encountered within the soil pit, and thus a limited number of sensors had to be confined in the smallest possible volume.

All the sensors that could be installed in either orientation were investigated in both vertical and horizontal orientations. Hereafter, the four combinations of soil type and sensor orientation are referred to as silt loam H (for horizontal), silt loam V (for vertical), loamy sand H, and loamy sand V. For horizontal sensor orientation, soil pits were dug at both sites such that the four walls of the pits were perpendicular to the ground surface. We ensured that the soil beyond the cuboidal pits was undisturbed and the soil structure was maintained. In the silt loam soil, the pit was dug between two maize rows, whereas in the loamy sand, the pit was dug in a representative grassed area.

For silt loam H and loamy sand H, the sensors were installed in one of the pit walls parallel to the ground surface at 60 cm from the soil surface, such that the sensing components (prongs, ceramic disks, etc.) were completely embedded in undisturbed soil and all measurements were taken in undisturbed soil. The 60 cm depth was selected to avoid spatially heterogeneous wetting patterns at shallower depths and due to its coincidence with the effective root volume. Sensor outputs are very sensitive to the effectiveness of sensor installation, necessitating that the installation procedure is conducted with extreme caution. The inter-sensor distance was maintained in such a way that the sensors' volumes of influence did not overlap and were independent, which was achieved by including a safety factor. Following the sensor installation, the pit was refilled with the same volume of soil, ensuring appropriate compaction (replicating original conditions), and the same soil layers were replaced at their original depths to reconstruct the original soil profile.

For silt loam V and loamy sand V, the sensors were installed perpendicular to the ground surface by pushing the sensors into the soil layer such that the sensing components were placed in undisturbed soil. The sensors in vertical orientation were installed such that the geometric midpoints of the sensing components were in the same horizontal plane in an effort to make fair comparisons across sensors with varying probe lengths and thus varying sensing volumes. For silt loam V, the horizontal plane was 30 cm below the ground surface. For loamy sand V, the horizontal plane was 50 cm below the ground surface (deeper due to the higher infiltration rates in loamy sand than in silt loam).

The installation was a more crucial task for the silt loam site because the sensors had to be in the root zone of the row crop, which was not as much a concern for the loam sand (grassland) site. Thus, for silt loam H, the sensors were directly under the plant row within the root zone, and for silt loam V the sensors were installed in the inter-plant spacing, ensuring that the root zone was monitored. Installation orientation remains an open question, as most commercial sensors are often recommended (by the manufacturer) to be installed in either orientation, without much discussion of how different orientations can impact soil moisture measurement.

The JD probe was the only multi-depth probe investigated in this research and hence had installation specifications different from those discussed above. Installation orientation is not a question associated with the JD probe. The JD probes were compared to the NP soil moisture at the five depths where the capacitors are located, i.e., 10, 20, 30, 50, and 100 cm. These depths are alterable, but the manufacturer default depths were used in this research. The capacitors are encased in plastic tubes, which were permanently placed in the soil throughout the growing season. The JD probes were wet installed (i.e., with the use of a slurry) using a handheld auger, following the manufacturer recommendations.

Two NP access tubes were installed at each site for reference soil moisture data collection. The placement of these tubes was such that they were in the immediate vicinity of the sampling area (within 0.5 m) of the sensors to be evaluated. For example, in silt loam, the NP access tubes were installed in the same row as the other sensors, which ensured fair assessments. The access tubes were kept covered at all times, except at the time of measurement, to ensure no interaction of external moisture. All the sensors as well as the NP access tubes remained in the soil throughout the two calendar years to maintain consistency and minimize soil disturbance.

Data Collection and Measurements

All the sensors were programmed to read soil moisture status every minute and output hourly averages throughout the two growing seasons at the two sites. Each of the sensors was equipped with a data logger that recorded hourly sensor data until the datasets were retrieved manually, except for the JD probe, for which telemetry was used for data retrieval. Each of the sensors was used with data loggers that were manufacturer-recommended, although provisions can be made to use a single datalogger, e.g., CR10X, with all the sensors (Irmak and Haman, 2001; Jabro et al., 2018). This course of action aimed to represent the equipment that would be used by producers and other end-users in commercial field conditions. The NP measurements were conducted in both access tubes at the two sites on a weekly frequency throughout the two growing seasons. For each access tube, eight neutron count measurements were conducted each week, one for each depth where various sensors were installed, i.e., 10 cm (JD probe), 20 cm (JD probe), 30 cm (JD probe and all sensors in silt loam V), 50 cm (JD probe and all sensors in loamy sand V), 60 cm (all sensors in silt loam H and loamy sand H), and 100 cm (JD probe).

Statistical Analyses

The soil moisture sensor outputs (sensor-measured θ_v) were compared with NP-measured θ_v (θ_{vref}) using certain statistical measures, i.e., root mean squared error (RMSE, m^3 m^{-3}) and mean bias error (MBE, m^3 m^{-3}):

$$\mathrm{RMSE} = \sqrt{\frac{\sum_{i=1}^{n}\left(E_i - M_i\right)^2}{n}} \tag{6}$$

$$\mathrm{MBE} = \frac{1}{n}\sum_{1}^{n}\left(M_i - E_i\right) \tag{7}$$

where M_i is the sensor-measured θ_v, E_i is the corresponding NP-measured θ_{vref}, and n is the number of observations. Each observation from a sensor was an hourly mean value, corresponding to the hour when θ_{vref} was measured. For sensor evaluation and calibration, n ranged from 15 to 20 depending on the site and sensor (table 3), while n was 12 for validation (in 2018).

MBE was used to interpret the nature of the error associated with the sensor-measured θ_v with respect to θ_{vref}. An MBE of zero implies that θ_v and θ_{vref} are unbiased, while positive and negative values of MBE imply that θ_v is overestimating and underestimating θ_{vref}, respectively. RMSE was used to denote the absolute value of the error that would be associated with θ_v. Pairwise soil moisture data from the sensors in question and the NP (θ_v and θ_{vref}, respectively) from the 2017 growing season were used in an ordinary least squares (OLS) regression analysis to quantitatively assess the performance of each sensor in the two soil types and orientations. To statistically infer if sensor performance varied by soil type, installation orientation, and the choice of sensor, we used the slopes (m) and intercepts (c) of the θ_v versus θ_{vref} regressions as observations to conduct a three-way ANOVA. We used the resulting p-values to infer if these factors were responsible for differences in performance. Additionally, coefficient of determination (R^2), standard error (SE) of m, and confidence interval (CI) of m (at 95% and 99% significance levels) were determined from the following equation:

$$\theta_v = m \times \theta_{vref} \left(\pm \mathrm{SE}\right) + c \tag{8}$$

The RMSE and MBE calculated from absolute values of θ_v as calculated above do not allow fair comparisons of sensor performance across the two soil types. To allow this comparison, θ_v was represented as a relative function of soil-specific field capacity and permanent wilting point by calculating the percent transpirable soil water (eq. 9):

$$\mathrm{PTSW}\ (\%) = \frac{\left(\theta_v - \mathrm{PWP}\right)}{\left(\mathrm{Field\ capacity} - \mathrm{PWP}\right)} \times 100 \tag{9}$$

where PTSW is the percent transpirable soil water, and PWP is permanent wilting point.

Sensor Performance Assessment, Calibration, and Validation

The θ_v and θ_{vref} data from 2017 were used to assess the sensors using the statistical indicators listed in the previous section. Each sensor was characterized for its performance to reflect true soil moisture conditions primarily using RMSE and MBE. While the sensors were evaluated for their accuracy using RMSE and MBE, they were also evaluated for their precision using R^2 and CI primarily. The m and c from the regression analysis were used to develop calibration equations for each sensor. Each sensor was ranked for its accuracy and precision using RMSE and R^2 as criteria, respectively, with the aim of providing an objective method for selecting one sensor over another by the user. Once the calibration functions were developed for each sensor in each soil type, the functions were applied to the original sensor-measured θ_v obtained independently during the 2018 growing season. Hence, the original θ_v estimates and post-calibration θ_v estimates were compared to the independent NP-measured θ_{vref} from 2018 to investigate the effectiveness and repeatability of the calibration functions developed to improve the performance of each sensor in different conditions. If an improvement was detected, it was established that S.S.C. resulted in a performance benefit over F.C. This improvement was quantified as the difference in RMSE obtained under F.C. and S.S.C. relative to that under F.C. and hereafter is referred to as I_{RMSE}.

Sensitivity of Sensor Performance to Soil Temperature

Each sensor was evaluated for the influence of soil temperature on its performance when installed in the soil for prolonged periods of time, which exposed the sensor to a wide range of T_{soil}. To quantify this influence, the following linear regression was conducted:

$$D = \frac{\left(\theta_v - \theta_{vref}\right)}{\theta_{vref}} \times 100 = t \times T_{soil} + i \tag{10}$$

where D is the percentage deviation of θ_v from θ_{vref} for each measurement (percentage residuals), T_{soil} is the soil temperature (°C) to the time of measurement, t is the slope, and i is the intercept. The T_{soil} data were obtained from a CS655 sensor installed at each site. From this analysis, we tested if the slope of the relationship was statistically significant (at the 95% and 99% levels). The presence of a statistical significance implied that T_{soil} was shown to be affecting the performance of the sensor. For sensors where T_{soil} impacted sensor performance, the slope was used to interpret the nature of the change in performance with increasing T_{soil}. Moreover, the R^2 value obtained from these relationships was interpreted as the variance in sensor performance that is explained by soil temperature changes.

Results and Discussion

Temporal Patterns in Volumetric Soil-Water Content

We started by investigating how well the sensors performed in replicating the θ_v pattern as observed in θ_{vref}. Figures 3 and 4 present the temporal distribution of θ_v during the 2017 growing season as measured by all the sensors, including NP, in the silt loam and loamy sand, respectively. In silt loam H, all sensors showed overestimation of θ_v compared to θ_{vref}, except TEROS 21 (MPS-6), which showed both under- and overestimation during the experimental period (fig. 3a). While all the overestimating sensors showed θ_v between 0.3 and 0.6 $m^3\ m^{-3}$, CS616 substantially overestimated θ_{vref} and showed θ_v in a very high (and unrealistic) range of 0.65 to 0.95 $m^3\ m^{-3}$. Similarly, in loamy sand H (fig. 4a), all the sensors overestimated θ_{vref}, and most of the sensors were in the range of 0.02 to 0.12 $m^3\ m^{-3}$. However, three sensors (EC-5, 10HS, and TEROS 21) largely overestimated θ_{vref} beyond a

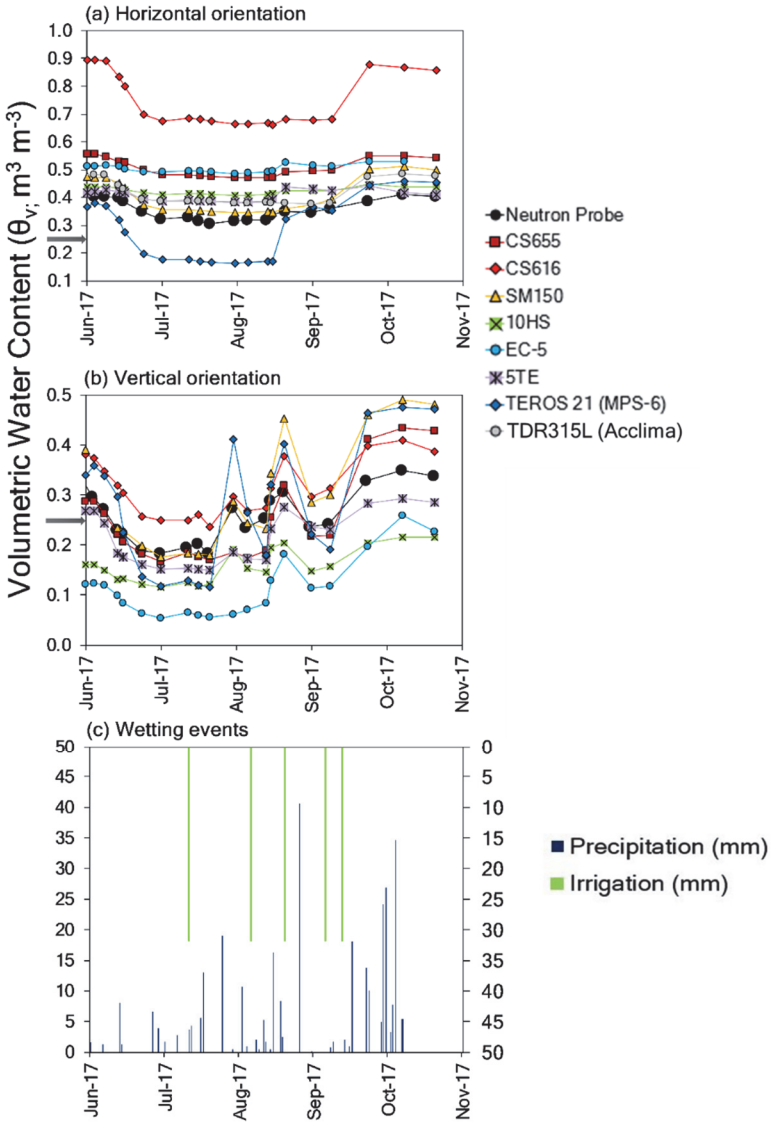

Figure 3. Distribution of volumetric soil water content (θ_v) measured by the soil moisture sensors during the experimental period in the silt loam soil in (a) horizontal orientation (60 cm depth) and (b) vertical orientation (30 cm depth), and (c) distribution and magnitude of wetting events, including both precipitation and irrigation. The gray arrow on the *y*-axes represents the soil-specific readily available soil-water.

reasonable range of error. Such soil moisture status (>0.13 m^3m^{-3}) is practically impossible in these soils and indicates poor performance of the sensors in their original F.C. conditions. Across both soils, the extent of θ_{vref} overestimation varied substantially across sensors as well as time. For example, TEROS 21 (MPS-6) in silt loam V underestimated θ_v prior to September, but overestimated thereafter. This implies that the patterns of over- and underestimation were not entirely systematic for a given sensor, which is unlike the findings of some research that was conducted in controlled laboratory conditions (Irmak and Irmak, 2005; Kizito et al., 2008; Vaz et al., 2013; Varble and Chávez, 2011).

The patterns of θ_v overestimation that were observed for the horizontal orientation changed in the vertical orientation (figs. 3b and 4b). This implies that orientation of the sensor can affect the performance statistics with respect to NP measurements. These differences can also be a consequence of differences in the actual volume of soil that is sampled when sensors are installed horizontally or vertically. For example, sensors such as CS655 have a cylindrical volume of influence with both major and minor axes. The volume of influence encounters more vertical volume in the V orientation and more horizontal volume in the H orientation. Thus, the patterns of moisture dynamics can vary in these differently aligned volumes, while the NP sampling volume is static, which can cause differences in the performance statistics. Interestingly, in silt loam V, all the sensors performed within a relatively narrow range of error, while in loamy sand V, TEROS 21 (MPS-6), similar to loamy sand H, presented very high θ_v throughout the 2017 monitoring period.

All sensors responded well to the wetting events at the silt loam site (both irrigation and precipitation events) and loamy sand site (precipitation only). Figures 3c and 4c present the timing and magnitude of the wetting events during the 2017 growing season. This response of θ_v to wetting was different for V and H sensors, not because of the orientation but because of the depths at which the sensors were installed. The H sensors at both sites were installed at deeper depths than the V

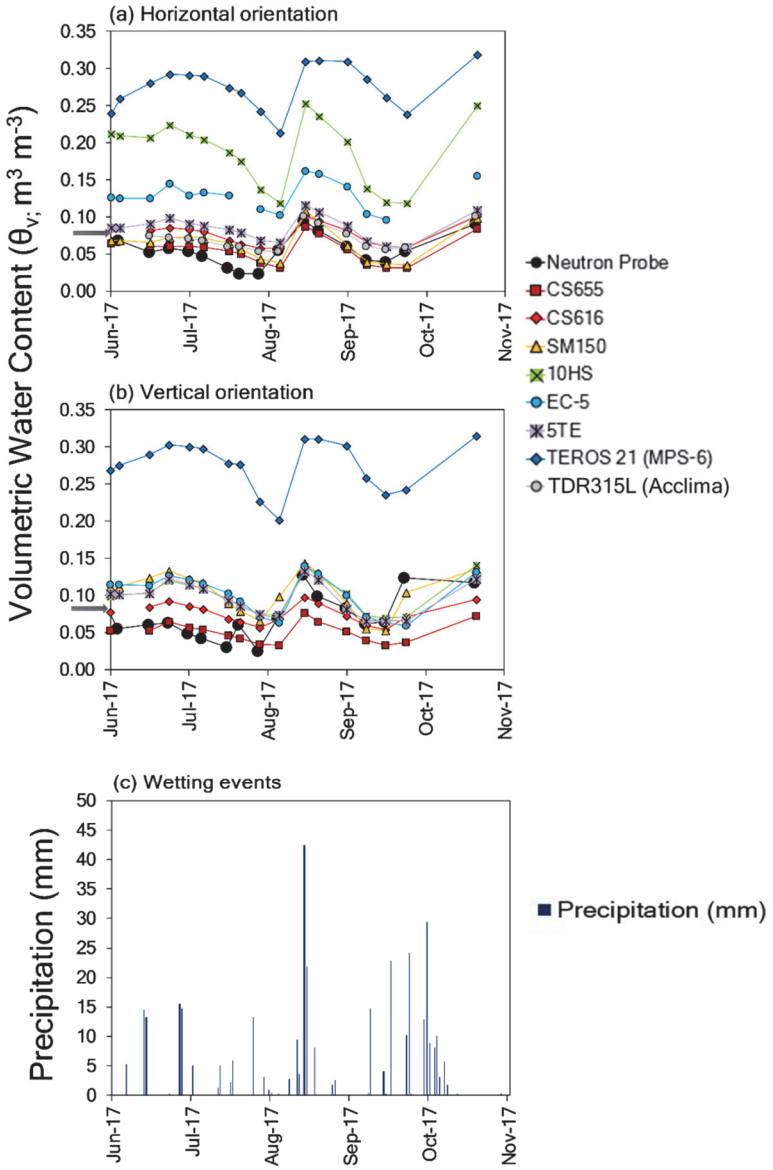

Figure 4. Distribution of volumetric soil-water content (θ_v) measured by the soil moisture sensors during the experimental period in the loamy sand soil in (a) horizontal orientation (60 cm depth), and (b) vertical orientation (50 cm depth), and (c) distribution and magnitude of precipitation. The gray arrow on the *y*-axes represents the soil-specific readily available soil-water.

sensors, which resulted in the wetting front reaching the volume of influence of the V sensors even with smaller wetting events, unlike the H sensors, which only responded to greater wetting events. However, this difference in θ_v response between H and V sensors was less pronounced at the loamy sand site due to greater infiltration rates. Thus, through qualitative assessment of the temporal patterns of θ_v, it is established that sensor performances are sensor-specific and soil-specific and show variation between the two orientations.

Impacts on Sensor Performance of Soil Type and Sensor Orientation

We found that the slopes and intercepts were statistically different (table 2) between the two soil types (at 99% and 90% confidence intervals). The slopes were statistically different among sensors (at 90% CI), while the intercepts were not. Both the slopes and intercepts were not statistically different between the two orientations. There was a significant interaction among soil type and sensor type (at 95% CI), while no interaction was observed in soil type and orientation. Installation orientation is a critical decision to make at the field level due to its role in conveying the geometry of the sampled volume for soil water status, and both orientations (H and V) can be of interest to the user, depending on the intention and objectives. While installation orientation is

Table 2. The p-values resulting from three-way ANOVA among soil type, sensor type, and installation orientation. The slope and intercept of the calibration equations for each sensor in the two soil types and two orientations were treated as observations for this analysis.

	p-Value	
Source of Variation	Slope	Intercept
Soil type	0.004	0.072
Sensor type	0.091	0.337
Orientation	0.321	0.445
Interaction: Soil type × Sensor type	0.045	0.041
Interaction: Soil type × Orientation	0.197	0.341

also a strong function of the sensor type used, a vast majority of soil moisture sensors are designed to be installed vertically. From our experimental framework, we did not find any detectable differences in sensor performance that are attributable to orientation. This might be a consequence of the framework's limited investigative capability due to the lack of replications among each orientation and soil type. Due to the potential impacts (that were inconclusive in this experiment) resulting from orientation, and the ease and avoidance of labor involved with one orientation over the other, a greater number of replicates should be used in a similar setup (in future research) to evaluate if one orientation is preferable to the other. The lack of replicates, which is admittedly a weakness of this study, may pose challenges to detecting differences in sensor performance due to orientation, although the soil type and sensor type were clearly recognized as influencers of soil moisture estimation performance.

Based on the abovementioned findings, the focus of our inferences and discussions hereafter is solely on the H orientation, as the sensor orientation was not a statistically significant factor. Ideally, the presence of no statistical significance would suggest pooling of the H and V orientation results; however, that is not a justified strategy in this particular context. As mentioned earlier, the H and V oriented sensors monitored different depths that were subject to different moisture conditions, which prevented us from pooling these datasets, as this would be unjustified. Due to the different moisture regimes experienced by the H and V oriented sensors as a consequence of their deployment at different depths, the θ_v versus θ_{vref} regressions showed distinct data clouds (data not shown). Thus, we selected the H orientation for further analyses and interpretation due to the fact that the major axes of the sensors' sampling volumes were aligned in the horizontal soil cross-section, which encountered relatively lower spatial variability than the V orientation. In addition, by selecting the H orientation, we also ensured that our findings are comparable to the literature, as most previous studies have evaluated sensors installed in the H orientation.

The sensor-specific OLS functions that were developed are presented in figure 5 (silt loam) and figure 6 (loamy sand) for all horizontally oriented sensors except the JD probe. Due to its multiple depths of measurement, the OLS functions for the JD probe are presented in figure 7 (silt loam) and figure 8 (loamy sand). The performance assessment was conducted for two desirable characteristics expected from an ideal sensor, i.e., precision and accuracy.

Precision-Based Performance Assessment

The coefficient of determination (R^2) was used to indicate the precision demonstrated by the sensors. Hence, precision in the context of this research refers to the degree to which the sensors were able to explain the variance observed in true

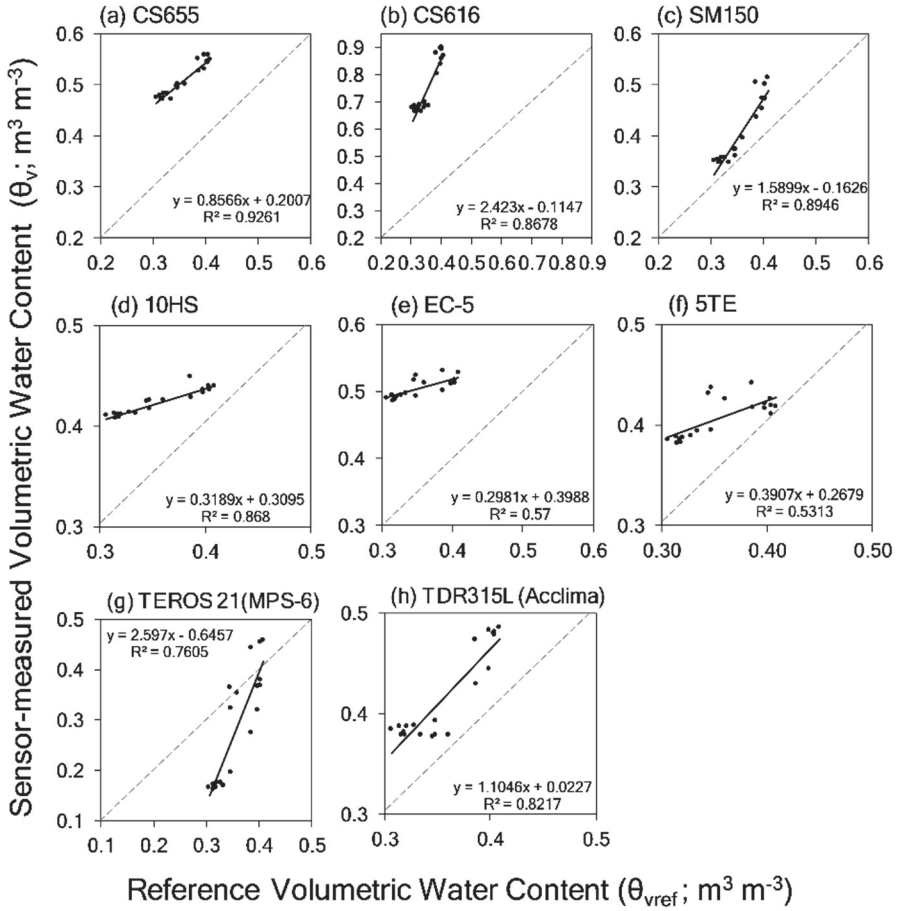

Figure 5. Linear regression among sensor-measured volumetric soil water content (θ_v) and reference volumetric soil water content (θ_{vref}) for (a) CS655, (b) CS616, (c) SM150, (d) 10HS, (e) EC-5, (f) 5TE, (g) TEROS 21 (MPS-6), and (h) TDR-315L sensors in silt loam soil in horizontal orientation. The function and coefficient of determination (R^2) included in each curve represent the linear fit trendline.

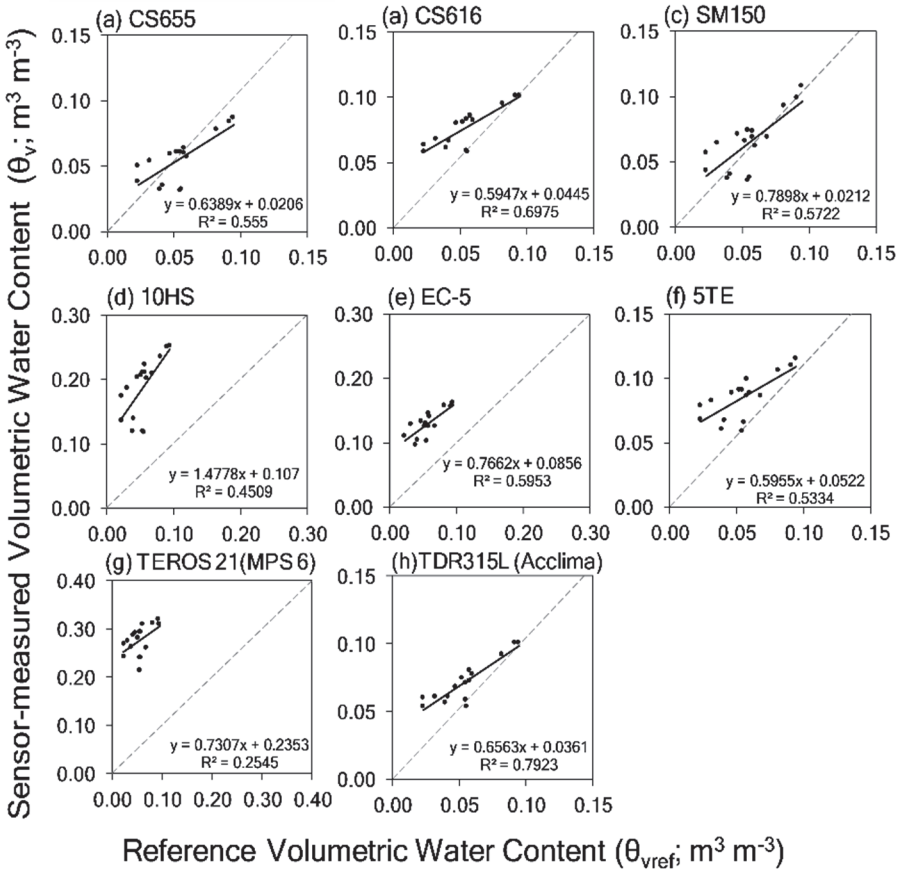

Figure 6. Linear regression among sensor-measured volumetric soil water content (θ_v) and reference volumetric soil water content (θ_{vref}) for (a) CS655, (b) CS616, (c) SM150, (d) 10HS, (e) EC-5, (f) 5TE, (g) TEROS 21 (MPS-6), and (h) TDR-315L sensors in loamy sand soil in horizontal orientation. The function and coefficient of determination (R^2) included in each curve represent the linear fit trendline.

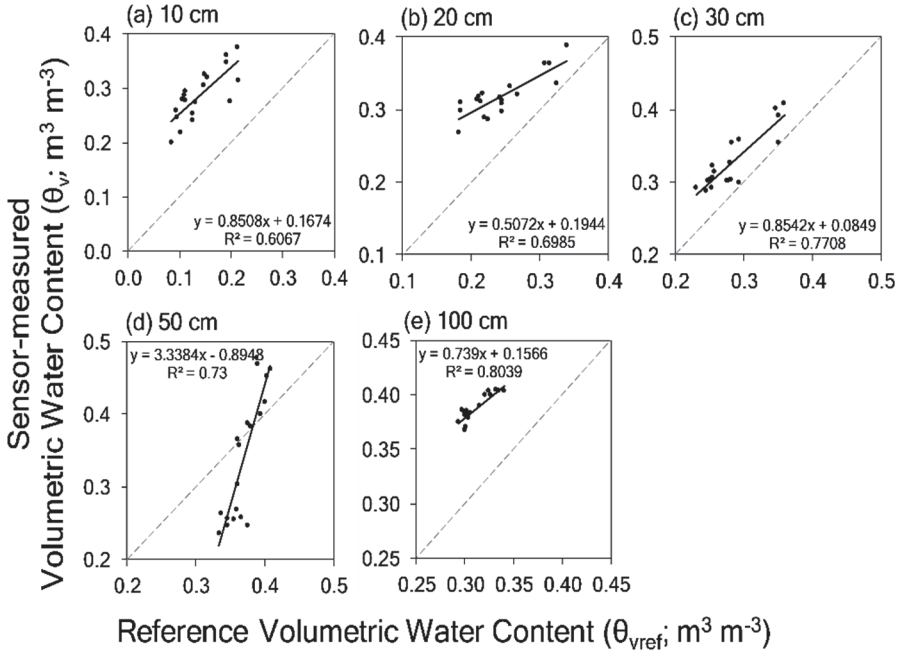

Figure 7. Linear regression among JD probe-measured volumetric soil water content (θ_v) and reference volumetric soil water content (θ_{vref}) for (a) 10 cm, (b) 20 cm, (c) 30 cm, (d) 50 cm, and (e) 100 cm depths in silt loam soil. The function and coefficient of determination (R^2) included in each curve represent the linear fit trendline.

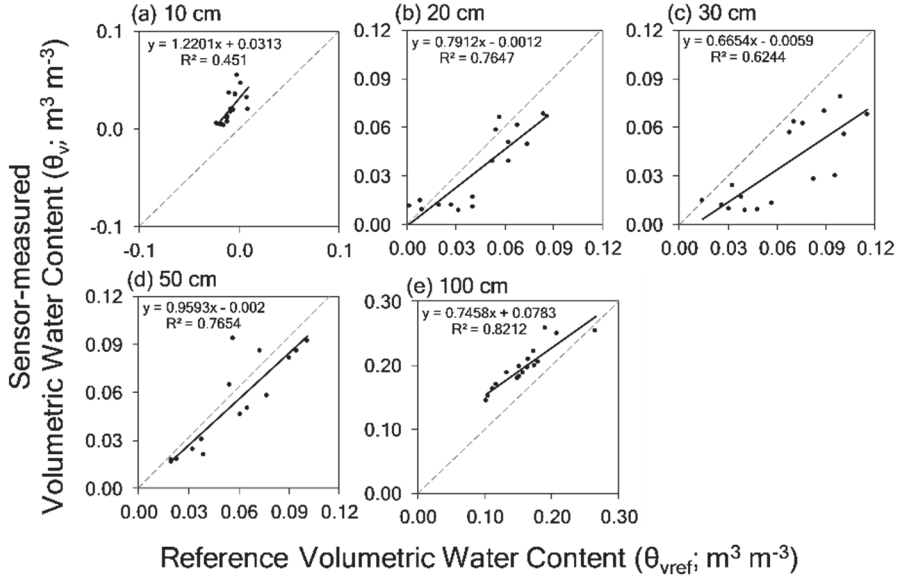

Figure 8. Linear regression among JD probe-measured volumetric soil water content (θ_v) and reference volumetric soil water content (θ_{vref}) for (a) 10 cm, (b) 20 cm, (c) 30 cm, (d) 50 cm, and (e) 100 cm depths in loamy sand soil. The function and coefficient of determination (R^2) included in each curve represent the linear fit trendline.

θ_{vref}. Precision is a highly desirable characteristic for a sensor. High precision demonstrated by a sensor means high potential for application of the sensor, even though it is inaccurate, if appropriate S.S.C. is employed. In silt loam, CS655 ($R^2 = 0.93$) and 5TE ($R^2 = 0.53$) were the most and least precise sensors, respectively. Table 3 lists the R^2 values and rankings of all the sensors based on precision (the highest R^2 is rank 1). In loamy sand, TDR-315L and TEROS 21 (MPS-6) were the most and least precise sensors, with R^2 of 0.79 and 0.25, respectively. Moreover, in general, the sensors showed higher precision in silt loam ($R^2 = 0.53$ to 0.93) than in loamy sand ($R^2 = 0.05$ to 0.79). This might be due to differences in infiltration rate between the two soils. Due to higher hydraulic conductivity and infiltration rates in loamy sand, the moisture conditions are generally more transient, resulting in lower precision in loamy sand soils.

The JD probe is a multi-depth sensor probe (10, 20, 30, 50, and 100 cm), and its usage is not a function of installation orientation. For the rankings presented in table 3, only one depth of the JD probe (30 cm at the silt loam site and 50 cm at the loamy sand site) was used to be consistent with the depths of the other sensors. However, we also addressed the performance of the JD probe at each of its depths. Figures 7 and 8 present regression curves between θ_v and θ_{vref} at each of the five depths for the silt loam and loamy sand soils, respectively. Table 4 lists depth-specific quantitative assessment parameters estimated for the JD probe. The R^2 varied from 0.61 to 0.80 in silt loam and from 0.45 to 0.82 in loamy sand. There was no consistent pattern of relative precision differences among the two soil types across all depths. At both sites, the shallowest depth (10 cm) showed the lowest precision, which is because the accuracy of NP is

Table 3. Statistical indicators derived from comparison of sensor-measured volumetric soil water content (θ_v) and reference volumetric soil water content (θ_{vref}) measured in silt loam and loamy sand soils with horizontal sensor orientation.

Soil	Statistic	CS655	CS616	SM150	10HS	EC-5	5TE	TEROS 21 (MPS-6)	TDR-315L	JD Probe
Silt loam	RMSE ($m^3\ m^{-3}$)	0.15	0.4	0.06	0.07	0.15	0.06	0.11	0.06	0.05
	MBE ($m^3\ m^{-3}$)	0.15	0.39	0.05	0.07	0.12	0.05	-0.07	0.06	0.04
	Standard error ($m^3\ m^{-3}$)	0.01	0.04	0.02	0	0.01	0.01	0.06	0.02	0.02
	No. of observations	20	20	20	20	19	20	20	20	19
	R^2	0.93	0.87	0.89	0.87	0.57	0.53	0.76	0.82	0.77
	Significance level	0.99	0.99	0.99	0.99	0.99	0.99	0.99	0.99	0.99
	CI ($\alpha = 0.05$)	0.14	0.19	0.17	0.19	0.44	0.47	0.28	0.23	0.28
	CI ($\alpha = 0.01$)	0.19	0.26	0.23	0.26	0.61	0.64	0.38	0.32	0.38
	Rank (based on precision)	1	4	2	3	8	9	7	5	6
	Rank (based on accuracy)	5	6	2	3	5	2	4	2	1
Loamy sand	RMSE ($m^3\ m^{-3}$)	0.01	0.03	0.02	0.14	0.09	0.03	0.22	0.02	0.01
	MBE ($m^3\ m^{-3}$)	0.001	0.02	0.01	0.13	0.06	0.03	0.22	0.02	-0.004
	Standard error ($m^3\ m^{-3}$)	0.01	0.01	0.01	0.04	0.01	0.01	0.03	0.01	0.02
	No. of observations	16	16	17	17	15	17	17	16	15
	R^2	0.56	0.70	0.57	0.45	0.60	0.53	0.25	0.79	0.77
	Significance level	0.99	0.99	0.99	0.99	0.99	0.99	0.99	0.99	99%
	CI ($\alpha = 0.05$)	0.51	0.38	0.48	0.61	0.49	0.51	-0.94	0.29	33%
	CI ($\alpha = 0.01$)	0.71	0.52	0.66	0.84	0.69	0.71	1.3	0.41	46%
	Rank (based on precision)	6	3	5	8	4	7	9	1	2
	Rank (based on accuracy)	1	3	2	5	4	3	6	2	1

Table 4. Statistical indicators derived from comparison of JD probe-measured volumetric soil-water content (θ_v) and reference volumetric soil-water content (θ_{vref}) measured in silt loam and loamy sand soils.

Soil	Statistic	10 cm	20 cm	30 cm	50 cm	100 cm	Pooled data
Silt loam	RMSE (m^3 m^{-3})	0.15	0.08	0.05	0.07	0.08	0.07
	MBE (m^3 m^{-3})	0.15	0.07	0.04	-0.03	0.08	0.03
	Standard error (m^3 m^{-3})	0.03	0.02	0.02	0.05	0.01	0.06
	No. of observations	19	19	19	19	17	55
	R^2	0.61	0.70	0.77	0.73	0.80	0.16
	Significance level	99%	99%	99%	99%	99%	99%
	CI ($\alpha = 0.05$)	41%	34%	28%	31%	27%	64%
	CI ($\alpha = 0.01$)	57%	46%	38%	43%	38%	85%
Loamy sand	RMSE (m^3 m^{-3})	0.03	0.02	0.03	0.01	0.04	0.03
	MBE (m^3 m^{-3})	0.03	-0.01	-0.03	-0.004	0.04	0.002
	Standard error (m^3 m^{-3})	0.01	0.01	0.02	0.02	0.01	0.03
	No. of observations	17	17	17	15	17	49
	R^2	0.45	0.76	0.62	0.77	0.82	0.88
	Significance level	99%	99%	99%	99%	99%	99%
	CI ($\alpha = 0.05$)	61%	31%	43%	33%	26%	11%
	CI ($\alpha = 0.01$)	84%	42%	59%	46%	36%	15%

compromised when measuring θ_v at shallower depths. At shallower depths, the NP volume of influence might not be completely contained in the soil, and neutrons can escape from the surface, especially in low soil moisture conditions, confounding the θ_{vref} estimates. This might also be true for the 20 cm depth, as the radius of the volume of influence can vary depending on the soil water content.

Accuracy-Based Performance Assessment

Accuracy represents the performance of a sensor in being reflective of the θ_{vref} magnitude. In many cases, accuracy can be more important than precision, especially if the sensor is to be used under F.C., and it directly impacts the decision-making effectiveness. We used RMSE to denote the magnitude of accuracy demonstrated by a given sensor. Because RMSE is an absolute measure of accuracy, we used MBE to denote the over- or underestimation exhibited by the sensors with respect to NP. Table 3 lists the RMSE and MBE values for each sensor in both soil types. Table 3 also lists the rankings of the sensors when they were compared based on accuracy (RMSE). For the silt loam, JD probe and CS616 were the most and least accurate soil moisture sensors, with RMSE values of 0.05 and 0.40 m^3 m^{-3}, respectively. For the loamy sand, CS655 and TEROS 21 (MPS-6) were the best and least accurate sensors, with RMSE values of 0.01 and 0.22 m^3 m^{-3}, respectively.

On average, RMSE values were 67% lower for the loamy sand than for the silt loam, except for TEROS 21 (MPS-6) and 10HS. This implies that the sensors performed with greater accuracy in the loamy sand than in the silt loam with F.C., which agrees with the findings of Zhu et al. (2019) from their experiments conducted under controlled laboratory conditions with 5TE, TDR300, CS616, 10HS, and SM150 sensors. They also found that 5TE (RMSE = 0.041 m^3 m^{-3}) and CS616 (RMSE = 0.014 m^3 m^{-3}) were the most accurate sensors in silt loam and loamy sand soils among the sensors investigated. This is very similar to our findings, with slight differences in the RMSE values observed. The RMSE values (table 3) observed in our experiments were slightly higher than those reported by Zhu et al. (2019), which is most likely a result of differences in the experimental conditions (laboratory vs. field). Nevertheless, the ranges of RMSE observed for both soils were quite similar between our research and Zhu et al. (2019). Observing the MBE, we found that most of the sensors overestimated θ_v in both the silt loam and loamy sand soils.

Table 5. Soil-specific accuracy assessment for nine sensors evaluated in this research using root mean squared error (RMSE) and mean bias error (MBE) based on percent transpirable soil water (PTSW).

	Silt Loam		Loamy Sand	
Sensor	RMSE (PTSW)	MBE (PTSW)	RMSE (PTSW)	MBE (PTSW)
CS655	100	100	10	1
CS616	266	263	18	16
TDR-315L	42	40	14	12
SM150	38	32	12	7
10HS	47	44	98	95
EC-5	101	100	52	52
5TE	38	33	24	21
TEROS 21 (MPS-6)	72	-50	159	158
JD probe	32	29	10	-3

A direct quantitative comparison of sensor performance in estimating θ_v across the two soil types is not fair, due to differences in critical water-relevant soil parameters. To this end, RMSE and MBE were calculated based on PTSW rather than θ_v (table 5), allowing robust inter-soil performance comparisons. It was observed that most sensors performed better in the loamy sand soil, with the exceptions of TEROS 21 (MPS-6) and 10HS. Sensor performance (based on RMSE) was on average 67% better in the loamy sand soil than in the silt loam soil. The highest inter-soil difference in performance was demonstrated by CS616 (93%), while the lowest difference was demonstrated by 5TE (37%). Moreover, the patterns of over- and underestimation of true PTSW by the different sensors were consistent across the two soil types, with the exception of TEROS 21 (MPS-6) and JD probe. While TEROS 21 (MPS-6) and JD probe underestimated and overestimated, respectively, in silt loam, these patterns were reversed in loamy sand. The remainder of the sensors maintained their patterns of overestimation in both soils.

Sensor Calibration and Validation

The parameters from the OLS regression functions (figs. 5 to 8) in their inversed form (θ_{vref} on *y*-axes, θ_v on *x*-axes) can be used as calibration functions to correct the systematic component of the error in θ_v. Tables 3 and 4 list the statistical significance of the slope of the OLS regression

and confidence intervals at 99% and 95% significance levels. The calibration functions presented in tables 6 and 7 were applied to the independent θ_v data from the 2018 growing season (referred to as S.S.C.). The resulting θ_v values were compared against the θ_{vref} measured using the NP in 2018, and the RMSE values were investigated for any improvement post-calibration (validation). Any detected improvement in RMSE was termed I_{RMSE}, which was calculated as the difference in RMSE under F.C. and S.S.C. as a percentage of RMSE under F.C.

Significant improvements were observed for most of the sensors after S.S.C. (table 8). An improvement in performance resulted only when ΔRMSE was positive; in these cases, ΔRMSE was referred to as I_{RMSE}. On average across all sensors, the use of S.S.C. resulted in I_{RMSE} (improvements in performance) magnitudes of 56% and 62% for silt loam and loamy sand, respectively (table 7). EC-5 and CS616 showed the highest I_{RMSE} (89%) in silt loam. In loamy sand, 10HS showed the highest I_{RMSE} (85%) post-calibration. We also ranked the sensors in table 8 based on their post-S.S.C. RMSE values. JD probe demonstrated post-calibration improvement of about 36% at all five depths in silt loam; however, in loamy sand, improvement was only achieved for the 10 cm and 100 cm sensors, with I_{RMSE} of 30% and 26%, respectively (table 9).

We also investigated I_{RMSE} by classifying the statistics based on the principle employed by the sensors to sense soil moisture. For this, we averaged the I_{RMSE} for the sensors in each category (i.e., TDR-based, capacitance-based, and ER-based). In silt loam, the TDR-based sensors showed the highest I_{RMSE} (72%), followed by the capacitance-based (44%) and ER-based (42%) sensors. However, for loamy sand, the ER-based sensors showed the highest I_{RMSE} of 88%. Other studies have suggested that S.S.C. led to improvement in the performance of soil moisture sensors relative to F.C. (Zhu et al., 2019; Heng et al., 2002; Datta et al., 2018; Mittelbach et al., 2012; Quinones et al., 2003; Brocca et al., 2007; Jabro et al., 2005; Evett and Steiner, 1995; Tedeschi et al., 2014), and our research supports those observations. However, our analysis also suggests that this improvement is subject to soil-specific differences. S.S.C. did not result in an overall performance improvement for the three sensor categories in loamy sand soil. Thus, S.S.C. is not necessary for all soil types, and in such cases F.C. results in reasonable performance. This is usually the case when sensors already perform at an acceptable accuracy under F.C. and any attempt to implement S.S.C. does

Table 6. Calibration functions proposed and goodness of fit (R^2) as derived from comparison of sensor-measured volumetric soil water content (θ_v) and reference volumetric soil water content (θ_{vref}) measured in silt loam and loamy sand soils with horizontal orientation. In the calibration functions, *y* refers to site-specific calibrated θ_v, and *x* refers to factory calibrated θ_v.

Soil	Sensor	Calibration Function	R^2
Silt loam	CS655	$y = 1.0812x - 0.1906$	0.93
	CS616	$y = 0.3289x + 0.1103$	0.71
	SM150	$y = 0.5627x + 0.1292$	0.89
	10HS	$y = 2.7215x - 0.7951$	0.87
	EC-5	$y = 1.9119x - 0.6098$	0.57
	5TE	$y = 1.36x - 0.1969$	0.53
	TEROS 21 (MPS-6)	$y = 0.2928x + 0.2747$	0.76
	TDR-315L	$y = 0.7439x + 0.0469$	0.82
Loamy sand	CS655	$y = 0.8687x + 0.0062$	0.56
	CS616	$y = 1.1729x - 0.0358$	0.7
	SM150	$y = 0.7245x + 0.0082$	0.57
	10HS	$y = 0.3051x - 0.0024$	0.45
	EC-5	$y = 0.777x - 0.0434$	0.6
	5TE	$y = 0.8957x - 0.0211$	0.53
	TEROS 21 (MPS-6)	$y = 0.3483x - 0.0409$	0.25
	TDR-315L	$y = 1.2072x - 0.0323$	0.79

Table 7. Calibration functions proposed and goodness of fit (R^2) as derived from comparison of JD probe-measured volumetric soil water content (θ_v) and reference volumetric soil water content (θ_{vref}) at five soil depths measured in silt loam and loamy sand soils. In the calibration functions, *y* refers to site-specific calibrated θ_v, and *x* refers to factory calibrated θ_v.

Soil	Soil Depth (cm)	Calibration Function	R^2
Silt loam	10	$y = 0.7131x - 0.0644$	0.61
	20	$y = 1.3771x - 0.194$	0.70
	30	$y = 0.9023x - 0.0116$	0.77
	50	$y = 0.2187x + 0.2957$	0.73
	100	$y = 1.0879x - 0.1091$	0.80
Loamy sand	10	$y = 0.3696x - 0.0159$	0.45
	20	$y = 0.9665x + 0.0119$	0.76
	30	$y = 0.9384x + 0.0296$	0.62
	50	$y = 0.7979x + 0.0149$	0.77
	100	$y = 1.1011x - 0.0578$	0.82

Table 9. Root mean squared error (RMSE) under factory calibration (F.C.) and site-specific calibration (S.S.C.) derived from comparison of JD probe-measured volumetric soil-water content (θ_v) and reference volumetric soil-water content (θ_{vref}) measured at five depths in silt loam and loamy sand. Change recorded in RMSE post-calibration (ΔRMSE) and the resulting rankings of the sensors are also included.

		Soil depth (cm)				
Soil	Statistic	10	20	30	50	100
Silt loam	RMSE: 2018 (mm); F.C.	0.12	0.10	0.10	0.09	0.14
	RMSE: 2018 (mm); S.S.C.	0.09	0.08	0.06	0.06	0.06
	ΔRMSE (%)	26	21	40	39	55
Loamy sand	RMSE: 2018 (mm); F.C.	0.06	0.02	0.03	0.02	0.03
	RMSE: 2018 (mm); S.S.C.	0.04	0.02	0.04	0.02	0.02
	ΔRMSE (%)	30	-4	-19	-39	26

Table 8. Root mean squared error (RMSE) under factory calibration (F.C.) and site-specific calibration (S.S.C.) derived from comparison of sensor-measured volumetric soil-water content (θ_v) and reference volumetric soil-water content (θ_{vref}) in silt loam and loamy sand soils with horizontal orientation. Change recorded in RMSE post-calibration (ΔRMSE) and the resulting ranking of the sensors are also included.

Soil	Statistic	CS655	CS616	SM150	10HS	EC-5	5TE	TEROS 21 (MPS-6)	TDR-315L
Silt loam	RMSE: 2018 (mm); F.C.	0.17	0.5	0.1	0.09	0.4	0.07	0.09	0.1
	RMSE: 2018 (mm); S.S.C.	0.05	0.05	0.04	0.06	N/A	0.04	0.05	0.04
	ΔRMSE (%)	71	89	58	32	N/A	41	47	56
	Rank	6	7	4	8	N/A	1	5	3
Loamy sand	RMSE: 2018 (mm); F.C.	0.02	0.03	0.02	0.15	0.07	0.04	N/A	0.03
	RMSE: 2018 (mm); S.S.C.	0.02	0.02	0.02	0.02	0.02	0.01	N/A	0.02
	ΔRMSE (%)	-10	51	-3	85	79	65	N/A	28
	Rank	4	3	7	6	2	1	N/A	5

not yield better performance due to the possibility of overfitting of the calibration functions. In such situations, the systematic error is low and the random uncertainty proportion is high, resulting in no benefit when S.S.C. is applied. Thus, some factory-calibrated sensors (CS655, SM150, and JD probe in this research) demonstrated decreased performance post-S.S.C., and their use under F.C. in loamy sand soil holds reasonable potential, which was also supported by Jabro et al. (2018).

Impact of Temperature Variability on Sensor Performance

Because the sensors were installed at two field sites for two entire growing seasons, a wide range of soil temperatures (T_{soil}) was encountered. The T_{soil} range observed for silt loam and loamy sand were 14°C to 23°C and 14°C to 25°C, respectively, throughout the 2017 and 2018 growing seasons. In silt loam, the performance of CS655, 10HS, 5TE, and TEROS 21 (MPS-6) showed sensitivity to T_{soil} fluctuations (table 10), which was statistically significant (at 95% significance level). We found that in silt loam, T_{soil} was able to explain 17% of the variability observed in 10HS sensor performance (informed by R^2), which was the maximum among all sensors. TEROS 21 (MPS-6) had the highest sensitivity to T_{soil}, with a slope of -4.25. On the contrary, while statistically significant ($p < 0.05$), 5TE was the least sensitive to T_{soil} variability, with a slope of 1.81. In loamy sand, however, no statistically significant ($p > 0.05$) sensitivity was detected for any of the sensors. Our estimates of the sensitivity of sensor performance to T_{soil} fluctuations serve to discern sensors and soil conditions that can show performance differences when employed under variable T_{soil} conditions. Because θ_{vref} is unaffected by T_{soil} variability, the S.S.C. developed in this research implicitly also accounts for the T_{soil}-induced inaccuracy.

The application of soil moisture sensors in irrigation and other farm-related decision-making requires them to remain installed for the duration of the growing season, or for a longer period. In these situations, the diurnal and seasonal variations in air temperature, and hence soil temperature, have potential to affect the performance of the sensor, in addition to the intrinsic inaccuracy stemming from the underlying sensing mechanism. This effect of temperature has been shown to vary with the soil type, soil water content, and sensor type (Zhu et al., 2019; Kammerer et al., 2014; Czarnomski et al., 2005; Seyfried and Murdock, 2001; Evett et al., 2006; Or and Wraith, 1999).

Conclusions

The performance of nine commercial soil moisture sensors was evaluated in two different soils (silt loam and loamy sand) with two different installation orientations (vertical and horizontal). While the sensor type and soil type significantly affected the sensor performance in accurately estimating soil moisture, the sensor installation orientation did not play a role in sensor performance. Given this, we deduced our interpretations based on only the horizontal orientation for all sensors. We found that under F.C., the JD probe was the most accurate sensor in silt loam, while CS655 was found to be the best-suited sensor in loamy sand. An analysis of the percent transpirable soil water (PTSW) revealed that sensor performance was generally better in loamy sand than in silt loam. Overall, we concluded that under F.C., the CS655, CS616, 5TE, TDR-315L, and JD probe can be used in loamy sand with an accuracy (RMSE) range between 0.01 to 0.03 $m^3\ m^{-3}$. However, S.S.C. was beneficial in silt loam conditions. All sensors in the silt loam soil showed high I_{RMSE} that varied from 32% to 89%. Under S.S.C., the 5TE sensor in silt loam ranked highest in accuracy. On the other hand, in loamy sand, most of the sensors showed improved performances post-S.S.C., with I_{RMSE} varying from 28% to 85%.

This research presents quantitative information on the precision and accuracy observed in various sensors' expected performance in field conditions with two different soil types. We used quantitative metrics to provide rankings of the sensors when considered for various applications in different conditions of use. The findings have high transferability in silt loam and loamy sand soils within the θ_{vref} and T_{soil} ranges investigated. The findings and resources of this research can inform different user groups to: (1) select the best-performing sensors for their operations and be aware of the inaccuracy encountered with sensor use, (2) evaluate if F.C. or S.S.C. results in appropriate performance, and (3) apply the developed S.S.C. functions for optimizing the use of a given sensor. The findings of these experiments have been used in consequent applications, including: (1) understanding how errors in sensing θ by sensors propagate to critical end-user oriented metrics like total soil water, evapotranspiration, and irrigation decisions (Sharma et al., 2021), and (2) addressing the operational feasibility of soil moisture sensors, to develop a framework to guide potential users to select best-suited sensors for both research and commercial applications (Kukal et al., 2020).

Table 10. Statistical indicators derived from the investigation of the sensitivity of sensor-performance to fluctuations in T_{soil} for each sensor under silt loam and loamy sand soils under horizontal installation orientation.

Soil	Statistic	CS655	CS616	SM150	10HS	EC-5	5TE	TEROS 21 (MPS-6)	TDR-315L
Silt loam	Slope	2.05	2.57	-0.75	2.06	0.68	1.81	-4.25	1.06
	R^2	0.12	0.05	0.02	0.17	0.02	0.16	0.13	0.05
	Significance level	95%	N.S.	N.S.	95%	N.S.	95%	95%	N.S.
Loamy sand	Slope	5.01	3.14	5.53	14.07	5.7	7.68	45.52	0.39
	R^2	0.06	0.01	0.05	0.03	0.01	0.05	0.17	0
	Significance level	N.S.	N.S.	N.S.	N.S.	N.S.	N.S.	N.S.	N.S.

ACKNOWLEDGEMENTS

This study is a part of a long-term research program that continues to investigate the fundamentals, performance, and feasibility of different soil moisture and soil properties measurement technologies in different soil types with various cropping systems in the Irmak Research Laboratory. Part of this long-term work presented in this article was included as part of the first author's MS study while she was a graduate student in the Irmak Research Laboratory at the University of Nebraska-Lincoln under the supervision of Suat Irmak. This project was partially supported by a grant obtained from the National Science Foundation (NSF) under Project No. CNS-1619285. Suat Irmak acknowledges the NSF and Irmak Research Laboratory members who assisted in this project. This research is partially based on work that is supported by the USDA National Institute of Food and Agriculture (Hatch Project No. NEB-21-155). Trade names of commercial products are provided solely for the information of the reader and do not constitute a recommendation by the authors or their institutions.

REFERENCES

Baumhardt, R. L., Lascano, R. J., & Evett, S. R. (2000). Soil material, temperature, and salinity effects on calibration of multisensor capacitance probes. *SSSA J., 64*(6), 1940-1946. https://doi.org/10.2136/sssaj2000.6461940x

Brocca, L., Morbidelli, R., Melone, F., & Moramarco, T. (2007). Soil moisture spatial variability in experimental areas of central Italy. *J. Hydrol., 333*(2-4), 356-373. https://doi.org/10.1016/j.jhydrol.2006.09.004

Caldwell, T. G., Bongiovanni, T., Cosh, M. H., Halley, C., & Young, M. H. (2018). Field and laboratory evaluation of the CS655 soil water content sensor. *Vadose Zone J., 17*(1), 170214. https://doi.org/10.2136/vzj2017.12.0214

Czarnomski, N. M., Moore, G. W., Pypker, T. G., Licata, J., & Bond, B. J. (2005). Precision and accuracy of three alternative instruments for measuring soil water content in two forest soils of the Pacific Northwest. *Canadian J. Forest Res., 35*(8), 1867-1876. https://doi.org/10.1139/x05-121

Datta, S., Taghvaeian, S., Ochsner, T. E., Moriasi, D., Gowda, P., & Steiner, J. L. (2018). Performance assessment of five different soil moisture sensors under irrigated field conditions in Oklahoma. *Sensors, 18*(11), 3786. https://doi.org/10.3390/s18113786

Delta-T. (2016). User manual for the SM150 soil moisture sensor, SM150-UM-1.1. Burwell, UK: Delta-T Devices.

Doorenbos, J., & Kassam, A. H. (1979). Yield response to water. Irrigation and Drainage Paper No. 33. Rome, Italy: United Nations FAO.

Evett, S. R. (2003). Soil water measurement by neutron thermalization. In *Encyclopedia of water science* (pp. 889-893). New York, NY: Marcel Dekker.

Evett, S. R., & Steiner, J. L. (1995). Precision of neutron scattering and capacitance type soil water content gauges from field calibration. *SSSA J., 59*(4), 961-968. https://doi.org/10.2136/sssaj1995.03615995005900040001x

Evett, S. R., Tolk, J. A., & Howell, T. A. (2003). A depth control stand for improved accuracy with the neutron probe. *Vadose Zone J., 2*(4), 642-649. https://doi.org/10.2136/vzj2003.6420

Evett, S. R., Tolk, J. A., & Howell, T. A. (2006). Soil profile water content determination: Sensor accuracy, axial response, calibration, temperature dependence, and precision. *Vadose Zone J., 5*(3), 894-907. https://doi.org/10.2136/vzj2005.0149

Evett, S., Laurent, J., Cepuder, P., & Hignett, C. (2002). Neutron scattering, capacitance, and TDR soil water content measurements compared on four continents. *Proc. 17th World Congress of Soil Science*, (pp. 14-21).

Giese, K., & Tiemann, R. (1975). Determination of the complex permittivity from thin-sample time domain reflectometry improved analysis of the step response waveform. *Adv. Molec. Relax. Proc., 7*(1), 45-59. https://doi.org/10.1016/0001-8716(75)80013-7

Hanson, B. R., & Peters, D. (2000). Soil type affects accuracy of dielectric moisture sensors. *California Agric., 54*(3), 43-47. https://doi.org/10.3733/ca.v054n03p43

Heng, L. K., Cayci, G., Kutuk, C., Arrillaga, J. L., & Moutonnet, P. (2002). Comparison of soil moisture sensors between neutron probe, Diviner 2000, and TDR under tomato crops. *Proc. 17th World Congress of Soil Science* (pp. 14-21).

Hignett, C., & Evett, S. (2008). Direct and surrogate measures of soil water content. IAEA-TCS-30. Vienna, Austria: International Atomic Energy Agency.

Irmak, S. (2010). Nebraska water and energy flux measurement, modeling, and research network (NEBFLUX). *Trans. ASABE, 53*(4), 1097-1115. https://doi.org/10.13031/2013.32600

Irmak, S. (2014). Plant growth and yield as affected by wet soil conditions due to flooding or over-irrigation. NebGuide G1904. Lincoln, NE: University of Nebraska Extension.

Irmak, S. (2015a). Inter-annual variation in long-term center pivot-irrigated maize evapotranspiration and various water productivity response indices: I. Grain yield, actual and basal evapotranspiration, irrigation-yield production functions, evapotranspiration-yield production functions, and yield response factors. *J. Irrig. Drain. Eng., 141*(5). https://doi.org/10.1061/(ASCE)IR.1943-4774.0000825

Irmak, S. (2015b). Inter-annual variation in long-term center pivot-irrigated maize evapotranspiration and various water productivity response indices: II. Irrigation water use efficiency, crop WUE, evapotranspiration WUE, irrigation-evapotranspiration use efficiency, and precipitation use efficiency. *J. Irrig. Drain. Eng., 141*(5). https://doi.org/10.1061/(ASCE)IR.1943-4774.0000826

Irmak, S. (2019a). Perspectives and considerations for soil moisture sensing technologies and soil water content- and soil matric potential-based irrigation trigger values. NebGuide 3045. Lincoln, NE: University of Nebraska Extension.

Irmak, S. (2019b). Soil-water potential and soil-water content concepts and measurement methods. EC3046. Lincoln, NE: University of Nebraska Extension.

Irmak, S., & Haman, D. Z. (2001). Performance of the watermark. Granular matrix sensor in sandy soils. *Appl. Eng. Agric., 17*(6), 787. https://doi.org/10.13031/2013.6848

Irmak, S., & Irmak, A. (2005). Performance of frequency-domain reflectometer, capacitance, and psuedo-transit time-based soil water content probes in four coarse-textured soils. *Appl. Eng. Agric., 21*(6), 999-1008. https://doi.org/10.13031/2013.20035

Irmak, S., Burgert, M. J., Yang, H. S., Cassman, K. G., Walters, D. T., Rathje, W. R., ... Teichmeier, G. J. (2012). Large-scale on-farm implementation of soil moisture-based irrigation management strategies for increasing maize water productivity. *Trans. ASABE, 55*(3), 881-894. https://doi.org/10.13031/2013.41521

Irmak, S., Payero, J. O., VanDeWalle, B., Rees, J. M., Zoubek, G. L., Martin, D., ... Leininger, D. (2016). Principles and operational characteristics of Watermark granular matrix sensor to measure soil water status and its practical applications for

irrigation management in various soil. EC783. Lincoln, NE: University of Nebraska Extension.
Jabro, J. D., Leib, B. G., & Jabro, A. D. (2005). Estimating soil water content using site-specific calibration of capacitance measurements from sentek EnviroSCAN systems. *Appl. Eng. Agric., 21*(3), 393-399. https://doi.org/10.13031/2013.18458
Jabro, J. D., Stevens, W. B., & Iversen, W. M. (2018). Field performance of three real-time moisture sensors in sandy loam and clay loam soils. *Arch. Agron. Soil Sci., 64*(7), 930-938. https://doi.org/10.1080/03650340.2017.1393528
Jacobsen, O. H., & Schjønning, P. (1993). A laboratory calibration of time domain reflectometry for soil water measurement including effects of bulk density and texture. *J. Hydrol., 151*(2), 147-157. https://doi.org/10.1016/0022-1694(93)90233-Y
Jones, S. B., Wraith, J. M., & Or, D. (2002). Time domain reflectometry measurement principles and applications. *Hydrol. Proc., 16*(1), 141-153. https://doi.org/10.1002/hyp.513
Kammerer, G., Nolz, R., Rodny, M., & Loiskandl, W. (2014). Performance of Hydra Probe and MPS-1 soil water sensors in topsoil tested in lab and field. *J. Water Resour. Prot., 6*(13), 1207. https://doi.org/10.4236/jwarp.2014.613110
Kelleners, T. J., Seyfried, M. S., Blonquist Jr., J. M., Bilskie, J., & Chandler, D. G. (2005). Improved interpretation of water content reflectometer measurements in soils. *SSSA J., 69*(6), 1684-1690. https://doi.org/10.2136/sssaj2005.0023
Kizito, F., Campbell, C. S., Campbell, G. S., Cobos, D. R., Teare, B. L., Carter, B., & Hopmans, J. W. (2008). Frequency, electrical conductivity, and temperature analysis of a low-cost capacitance soil moisture sensor. *J. Hydrol., 352*(3), 367-378. https://doi.org/10.1016/j.jhydrol.2008.01.021
Kukal, M. S., Irmak, S., & Sharma, K. (2020). Development and application of a performance and operational feasibility guide to facilitate adoption of soil moisture sensors. *Sustainability, 12*(1), article 321. https://doi.org/10.3390/su12010321
Leib, B. G., Jabro, J. D., & Matthews, G. R. (2003). Field evaluation and performance comparison of soil moisture sensors. *Soil Sci., 168*(6), 396-408. https://doi.org/10.1097/01.ss.0000075285.87447.86
Mittelbach, H., Lehner, I., & Seneviratne, S. I. (2012). Comparison of four soil moisture sensor types under field conditions in Switzerland. *J. Hydrol., 430-431*, 39-49. https://doi.org/10.1016/j.jhydrol.2012.01.041
Ochsner, T. E., Cosh, M. H., Cuenca, R. H., Dorigo, W. A., Draper, C. S., Hagimoto, Y., ... Zreda, M. (2013). State of the art in large-scale soil moisture monitoring. *SSSA J., 77*(6), 1888-1919. https://doi.org/10.2136/sssaj2013.03.0093
Ojo, E. R., Bullock, P. R., L'Heureux, J., Powers, J., McNairn, H., & Pacheco, A. (2015). Calibration and evaluation of a frequency domain reflectometry sensor for real-time soil moisture monitoring. *Vadose Zone J., 14*(3). https://doi.org/10.2136/vzj2014.08.0114
Or, D., & Wraith, J. M. (1999). Temperature effects on soil bulk dielectric permittivity measured by time domain reflectometry: A physical model. *Water Resour. Res., 35*(2), 371-383. https://doi.org/10.1029/1998WR900008
Paige, G. B., & Keefer, T. O. (2008). Comparison of field performance of multiple soil moisture sensors in a semi-arid rangeland. *JAWRA, 44*(1), 121-135. https://doi.org/10.1111/j.1752-1688.2007.00142.x
Plauborg, F., Iversen, B. V., & Lærke, P. E. (2005). *In situ* comparison of three dielectric soil moisture sensors in drip-irrigated sandy soils. *Vadose Zone J., 4*(4), 1037-1047. https://doi.org/10.2136/vzj2004.0138
Ponizovsky, A. A., Chudinova, S. M., & Pachepsky, Y. A. (1999). Performance of TDR calibration models as affected by soil texture. *J. Hydrol., 218*(1), 35-43. https://doi.org/10.1016/S0022-1694(99)00017-7
Quinones, H., Ruelle, P., & Nemeth, I. (2003). Comparison of three calibration procedures for TDR soil moisture sensors. *Irrig. Drain., 52*(3), 203-217. https://doi.org/10.1002/ird.95
Reynolds, S. G. (1970). The gravimetric method of soil moisture determination. *J. Hydrol., 11*(3), 258-273. https://doi.org/10.1016/0022-1694(70)90066-1
Romano, N. (2014). Soil moisture at local scale: Measurements and simulations. *J. Hydrol., 516*, 6-20. https://doi.org/10.1016/j.jhydrol.2014.01.026
Rüdiger, C., Western, A. W., Walker, J. P., Smith, A. B., Kalma, J. D., & Willgoose, G. R. (2010). Toward a general equation for frequency domain reflectometers. *J. Hydrol., 383*(3-4), 319-329. https://doi.org/10.1016/j.jhydrol.2009.12.046
Schmugge, T. J., Jackson, T. J., & McKim, H. L. (1980). Survey of methods for soil moisture determination. *Water Resour. Res., 16*(6), 961-979. https://doi.org/10.1029/WR016i006p00961
Seyfried, M. S., & Murdock, M. D. (2001). Response of a new soil water sensor to variable soil, water content, and temperature. *SSSA J., 65*(1), 28-34. https://doi.org/10.2136/sssaj2001.65128x
Sharma, K., Irmak, S., & Kukal, M. S. (2021). Propagation of soil moisture sensing uncertainty into estimation of total soil water, evapotranspiration, and irrigation decision-making. *Agric. Water Mgmt., 243*, article 106454. https://doi.org/10.1016/j.agwat.2020.106454
Tedeschi, A., Huang, C. H., Zong, L., You, Q. G., & Xue, X. (2014). Calibration equations for Diviner 2000 capacitance measurements of volumetric soil water content in salt-affected soils. *Soil Res., 52*(4), 379-387. https://doi.org/10.1071/SR13172
Topp, G. C., Davis, J. L., & Annan, A. P. (1980). Electromagnetic determination of soil water content: Measurements in coaxial transmission lines. *Water Resour. Res., 16*(3), 574-582. https://doi.org/10.1029/WR016i003p00574
Topp, G. C., Zegelin, S., & White, I. (2000). Impacts of the real and imaginary components of relative permittivity on time domain reflectometry measurements in soils. *SSSA J., 64*(4), 1244-1252. https://doi.org/10.2136/sssaj2000.6441244x
USDA. (2017). Census of agriculture. Washington, DC: USDA National Agricultural Statistics Service. Retrieved from https://www.nass.usda.gov/Publications/AgCensus/2017/
Varble, J. L., & Chávez, J. L. (2011). Performance evaluation and calibration of soil water content and potential sensors for agricultural soils in eastern Colorado. *Agric. Water Mgmt., 101*(1), 93-106. https://doi.org/10.1016/j.agwat.2011.09.007
Vaz, C. M., Jones, S., Meding, M., & Tuller, M. (2013). Evaluation of standard calibration functions for eight electromagnetic soil moisture sensors. *Vadose Zone J., 12*(2), 1-16. https://doi.org/10.2136/vzj2012.0160
Zazueta, F. S., & Xin, J. (1994). Soil moisture sensors. *Soil Sci., 73*, 391-401.
Zhu, Y., Irmak, S., Jhala, A. J., Vuran, M. C., & Diotto, A. (2019). Time-domain and frequency-domain reflectometry type soil moisture sensor performance and soil temperature effects in fine- and coarse-textured soils. *Appl. Eng. Agric., 35*(2), 117-134. https://doi.org/10.13031/aea.12908